Coherent Soliton States Hidden in Phase Space and Stabilized by Gravitational Incoherent Structures

Josselin Garnier,[1] Kilian Baudin,[2] Adrien Fusaro,[2,3] and Antonio Picozzi[2]
[1]*CMAP, CNRS, Ecole Polytechnique, Institut Polytechnique de Paris, 91128 Palaiseau Cedex, France*
[2]*Laboratoire Interdisciplinaire Carnot de Bourgogne, CNRS, Université Bourgogne Franche-Comté, 21078 Dijon, France*
[3]*CEA, DAM, DIF, F-91297 Arpajon Cedex, France*

(Received 14 February 2021; accepted 1 June 2021; published 30 June 2021)

We consider the problem of the formation of soliton states from a modulationally unstable initial condition in the framework of the Schrödinger-Poisson (or Newton-Schrödinger) equation accounting for gravitational interactions. We unveil a previously unrecognized regime: By increasing the nonlinearity, the system self-organizes into an incoherent localized structure that contains "hidden" coherent soliton states. The solitons are hidden in the sense that they are fully immersed in random wave fluctuations: The radius of the soliton is much larger than the correlation radius of the incoherent fluctuations, while its peak amplitude is of the same order of such fluctuations. Accordingly, the solitons can hardly be identified in the usual spatial or spectral domains, while their existence is clearly unveiled in the phase-space representation. Our multiscale theory based on coupled coherent-incoherent wave turbulence formalisms reveals that the hidden solitons are stabilized and trapped by the incoherent localized structure. Furthermore, hidden binary soliton systems are identified numerically and described theoretically. The regime of hidden solitons is of potential interest for self-gravitating Boson models of "fuzzy" dark matter. It also sheds new light on the quantum-to-classical correspondence with gravitational interactions. The hidden solitons can be observed in nonlocal nonlinear optics experiments through the measurement of the spatial spectrogram.

DOI: 10.1103/PhysRevLett.127.014101

Understanding the processes of self-organization in conservative Hamiltonian systems is a difficult problem that has generated significant interest. For nonintegrable wave systems, the formation of a coherent soliton state plays the role of a "statistical attractor" for the Hamiltonian system [1–4]. It is thermodynamically advantageous for the system to generate a large scale soliton, because this allows us to increase the amount of disorder ("entropy") in the form of thermalized small scale fluctuations [1–8].

The physical picture becomes more complex when the system exhibits long-range interactions, which dramatically slow down the thermalization process. A detailed understanding of this process is a subject of growing interest, in relation with peculiar features such as violent relaxation, ergodicity breaking, or inequivalence of thermodynamic ensembles [9]. In this respect, the Schrödinger-Poisson equation (SPE) (or Newton-Schrödinger equation) appears as a natural theoretical framework for studying a wave system with long-range interactions. The SPE was proposed with the aim of investigating quantum wave function collapse in the presence of a Newtonian gravitational potential [10,11]. Actually, the SPE may be obtained as the nonrelativistic limit of the self-gravitating Klein-Gordon equation [12,13] and, thus, describes the coupling of classical gravitational fields to quantum matter states. Soliton solutions of the SPE [14] have been used to introduce the concept of Bose stars [12,15]. More recently, the SPE has been proposed for a quantum mechanical formulation of dark matter that would solve the "cold dark matter crisis," e.g., the formation of a cusp in the classical description of cold dark matter [16–22]. Indeed, recent 3D numerical simulations of the SPE realized in the cosmological setting remarkably reveal that, as a rule, the system self-organizes into a large scale soliton core, which is surrounded by an incoherent structure that appears consistent with the classical description [23–30]. In other words, the repulsive quantum potential (arising from the uncertainty principle) that is inherent to the SPE leads to the formation of a solitonic core that solves the cusp problem of classical cold dark matter. This Bosonic model for dark matter is known in the literature as fuzzy-dark matter, ultralight axion dark matter, or Bose-Einstein condensate dark matter.

Our aim, in this Letter, is to unveil a previously unrecognized regime of the SPE. Considering a homogeneous initial condition, we show that, by increasing the amount of nonlinearity, the field evolves toward an incoherent localized state that contains "hidden" coherent soliton structures. The incoherent structure (IS) "hides" coherent soliton states in the following sense: (i) The soliton amplitude is of the same order as the fluctuations of the surrounding IS; (ii) The radius of the coherent soliton is larger than the correlation radius of the fluctuations of the IS, but smaller than the radius of the IS, see Eq. (3). Then, the coherent soliton state can hardly be identified in the usual spatial or spectral domains, while its existence is clearly unveiled in the phase-space representation. Our theory provides a detailed description of the hidden coherent soliton states, which remarkably reveals that they are trapped and stabilized by the surrounding IS. Aside from the SPE context, the hidden character of the solitons predicted here has not been discussed before in the soliton literature.

There is a surge of interest in studying analog gravity phenomena in optical laboratory-based experiments that recreate some aspects of the full gravitational system [31–36]. Gravity being inherently nonlinear and nonlocal, the hidden coherent soliton states predicted here could be observed in highly nonlocal nonlinear optics experiments [37–46], or alternatively in dipolar Bose-Einstein condensates [47].

Schrödinger-Poisson equation.—We consider a general form of the SPE in spatial dimension D

$$i\partial_t\psi = -\frac{\alpha}{2}\nabla^2\psi + V\psi, \tag{1}$$

$$\nabla^2 V = \gamma\eta_D|\psi|^2, \tag{2}$$

where $\alpha > 0$ and $\gamma > 0$ are the dispersion and nonlinear coefficients, with $\eta_1 = 2$, $\eta_2 = 2\pi$, $\eta_3 = 4\pi$. Accordingly, $V = -\gamma\int U_D(\boldsymbol{x}-\boldsymbol{y})|\psi(\boldsymbol{y})|^2 d\boldsymbol{y} \equiv -\gamma U_D * |\psi|^2$, with $U_1(x) = -|x|$, $U_2(\boldsymbol{x}) = -\log(|\boldsymbol{x}|)$, $U_3(\boldsymbol{x}) = 1/|\boldsymbol{x}|$. The SPE describes a Bose gas under its self-induced gravitational potential $V(\boldsymbol{x}, t)$ satisfying the Poisson Eq. (2) with $\alpha = \hbar/m$ and $\gamma = Gm/\hbar$, where m is the mass of the bosons and G the Newton gravitational constant.

Hidden soliton regime.—If we denote by $\bar{\rho}$ the typical amplitude of $|\psi|^2$ and by ℓ its typical radius, then $V \sim \gamma\bar{\rho}\ell^2$ and the characteristic nonlinear time scale is $\tau_{nl} = 1/(\gamma\bar{\rho}\ell^2)$. On the other hand, the time scale due to linear dispersion effects is $\tau_l = \lambda_c^2/(\alpha/2)$, where λ_c is the correlation radius of the field ψ. The healing length

$$\xi = \ell^{-1}[\alpha/(2\gamma\bar{\rho})]^{1/2},$$

then denotes the spatial scale such that linear and nonlinear effects are of the same order. The weakly nonlinear (kinetic) regime $\lambda_c \ll \xi$ (or $\tau_l/\tau_{nl} = \lambda_c^2/\xi^2 \ll 1$) is described by the recently developed wave turbulence (WT) kinetic theory [35,48]. This is not the regime addressed in this Letter.

It proves convenient to normalize the healing length $\tilde{\xi} = \xi/\Lambda$ with respect to the Jeans length $\Lambda = [\alpha/(2\gamma\bar{\rho})]^{1/4}$, which denotes the cut off spatial length below which a homogeneous wave is modulationally stable. The dimensionless parameter $\tilde{\xi} = \Lambda/\ell = (\xi/\ell)^{1/2}$ is directly related to a parameter $\Xi = (\hbar/m)^2/(2\ell^4\bar{\rho}G) = \tilde{\xi}^4$ that has been shown to control the quantum to classical limit, i.e., the Schrödinger-Poisson to Vlasov-Poisson correspondence in the limit $\hbar/m \to 0$ [27]. Indeed, for $\tilde{\xi} \lesssim 1$, the radius ℓ of a gravitational structure is of the same order as the healing length $\xi \sim \ell$, so that linear "quantum effects" play a fundamental role and the system exhibits a coherent dynamics that is essentially dominated by soliton structures. Massive numerical simulations in the cosmological setting have widely explored this regime [22–30]: They show the formation of an IS that is dominated in its center by a large amplitude coherent soliton peak ρ_S, typically much larger than the average density of the surrounding IS, $\rho_S \gg \bar{\rho}_{\mathrm{IS}}$, see [28]. Furthermore, the soliton radius R_S is typically of the order of the correlation radius of the fluctuations of the IS, $R_S \sim \lambda_c$ [23–27,29,49].

On the other hand, in the strongly nonlinear regime $\tilde{\xi} \ll 1$, the dynamics is dominated by the gravitational interaction described by the Vlasov-Poisson equation (VPE), which is a kinetic equation inherently unable to describe coherent soliton structures. In other words, in the regime $\tilde{\xi} \ll 1$ where $\alpha/\gamma \propto (\hbar/m)^2 \to 0$, coherent solitons should gradually disappear and the field $\psi(\boldsymbol{x}, t)$ should exhibit a purely incoherent dynamics featured by the generation of a large scale IS [27]. The main result in this Letter is to show that such an IS is not purely incoherent, but still contains hidden soliton states: The IS with typical average density $\bar{\rho}_{\mathrm{IS}}$, radius ℓ, and correlation radius λ_c, helps stabilizing a soliton of amplitude ρ_S and typical radius R_S verifying [50]

$$\lambda_c \sim \xi \ll R_S \sim \Lambda \ll \ell, \qquad \rho_S \sim \bar{\rho}_{\mathrm{IS}}. \tag{3}$$

More precisely, $R_S \sim \Lambda = \sqrt{\xi\ell}$ is the geometric average of ℓ and ξ. Note that the correlation radius is of the order of the de Broglie wavelength, $\lambda_c \sim \lambda_{\mathrm{dB}}$, where $\lambda_{\mathrm{dB}} \to 0$ in the quantum-to-classical (SPE to VPE) limit [27].

Simulations.—An example of the regime (3) is illustrated in Fig. 1. We consider SPE simulations in 1D because the parameter $\tilde{\xi}$ (or Ξ) does not depend on the spatial dimension D. The advantage with respect to 3D simulations is that much smaller values of the parameter Ξ can be reached in 1D. In Fig. 1, we consider $\Xi \simeq 5 \times 10^{-8}$, a value that appears inaccessible in 3D, where $\Xi > 10^{-4}$ [26,27,30]. In other words, the novel regime (3) seems out of reach of current 3D simulations [27].

The initial condition in Fig. 1 is a homogeneous wave $\psi(x, t = 0) = \sqrt{\bar{\rho}}$ with a superimposed small noise to initiate the modulational (gravitational) instability [54]. The instability is followed by a gravitational collapse, which is regularized by the formation of a virialized IS [23–29]. Note that the localized IS exhibits properties similar to those of incoherent optical solitons in nonlocal nonlinear media [39–41]. The IS in Fig. 1(a) does not exhibit apparent coherent soliton structures (also, see Movie 1 in [50]). This appears consistent with the SPE to classical VPE correspondence. Unexpectedly, however, the IS is not purely incoherent, but contains hidden coherent soliton

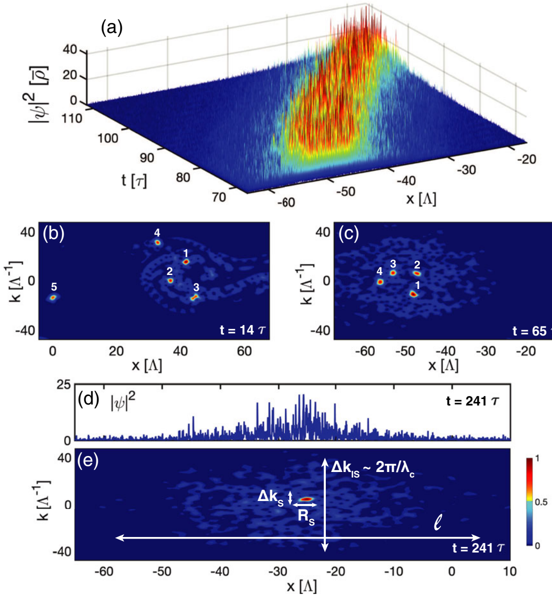

FIG. 1. Unveiling coherent solitons in phase space: SPE simulation for $\tilde{\xi} \simeq 1.5 \times 10^{-2}$: (a) Spatiotemporal evolution of the density $|\psi|^2(x,t)$. (b)–(c)–(e) The hidden solitons are unveiled in phase space by high intensity spots [labels (1)–(5)]. The number of solitons decreases with time, eventually leading to a single soliton (e). Density $|\psi|^2(x)$ (d) and corresponding phase-space portrait (e) at $t = 241\tau$, showing the separation of the three spatial scales $\lambda_c \sim 2\pi/\Delta k_{\mathrm{IS}} \ll R_S \sim 2\pi/\Delta k_S \ll \ell$, see Eq. (3). Parameters: $D = 1$ for $x \in [-L/2, L/2]$ with periodic boundary conditions ($L = 135\Lambda$, $\tau = 2\Lambda^2/\alpha$), see [50] and Movie 1.

structures. Such soliton entities are unveiled by a phase-space analysis of the field $\psi(x)$ provided by the Husimi representation (smoothed Wigner transform) [27,50], which denotes the field spectrum at different spatial positions. In optics, the Husimi transform is provided by the measurement of the spectrogram [55]. In phase space, the solitons are characterized by high intensity spots, while the surrounding small amplitude fluctuations denote the IS, see Fig. 1. The coherent soliton has a spectral width Δk_S much smaller than the spectral width of the IS, $\Delta k_{\mathrm{IS}} \gg \Delta k_S$, which means that the radius of the soliton, $R_S \sim 2\pi/\Delta k_S$, is much larger than the correlation radius $\lambda_c \sim 2\pi/\Delta k_{\mathrm{IS}}$ of the IS. Furthermore, remarking that $R_S \ll \ell$, we can clearly observe the separation of spatial scales (3) in Fig. 1(e).

The SPE simulations remarkably show that the hidden solitons get trapped by the IS, as revealed by the phase-space dynamics in Fig. 1. In particular, the untrapped soliton labeled “5” in Fig. 1(b) is not robust and disappears at $t \simeq 27\tau$, see Movie 1 in [50]. Then, the IS plays the role of an effective trapping potential for a soliton, as will be confirmed by the theory, see Eq. (6). The solitons hidden within the IS exhibit complex dynamics. Two solitons can spin around each other in phase space, thus, forming a binary system, see Fig. 2 and Movie 2 [50]. The number of solitons decreases with time, eventually leading to a single soliton that exhibits an ellipsoidal periodic motion in phase space, see Fig. 3 and Movie 3 [50].

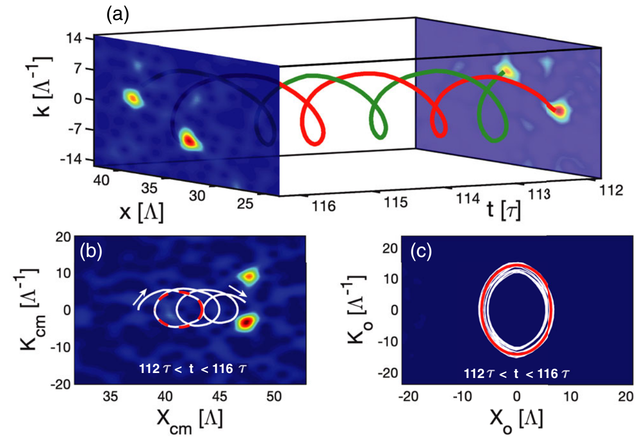

FIG. 2. Hidden binary soliton: (a) SPE simulation reported in Fig. 1 (at longer time) showing two solitons that orbit around each other in phase space. (b) The center of mass exhibits an ellipsoidal motion with period $\tau^{\mathrm{num}}_{\mathrm{c.m.}} \simeq 1.56\tau$ in agreement with the theory, see Eq. (8) [the horizontal shift is due to the motion of the IS, see Fig. 1(a)]. The dashed red line reports the theoretical ellipse $H_{\mathrm{c.m.}}$ from Eq. (7). (c) The spinning period of the solitons around each other $\tau^{\mathrm{num}}_{\mathrm{bin}} \simeq 1.43\tau$ is in agreement with the theory, see Eq. (10). The red line reports the theoretical prediction H_o from Eq. (9). See Movie 2 in [50].

Effective Schrödinger-Poisson equation.—We develop the theory in the general WT framework [4–8,39,56–61]. Because $\lambda_c \sim \xi$ [see Eq. (3)], the IS does not evolve in the weakly nonlinear regime [50]. It will be described by a WT-VPE that generalizes to long-range interactions [39], the WT Vlasov equation describing random waves in optics [37,39], hydrodynamics [58,62], or plasmas [63–65].

We describe the coupled coherent-incoherent dynamics of the soliton immersed in the IS by deriving a coupled system of SPE and WT-VPE. The soliton is characterized by a nonvanishing average $\langle\psi\rangle \neq 0$, so that the field can be decomposed into a coherent component $A(\boldsymbol{x}, t)$

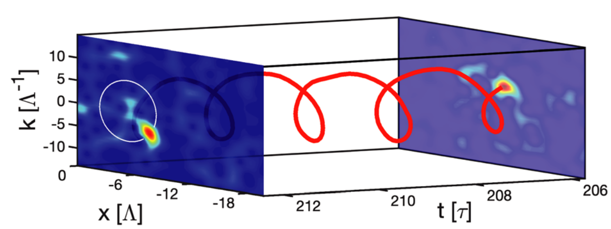

FIG. 3. Hidden single soliton: SPE simulation reported in Fig. 1 (at longer time) showing the phase-space evolution of a single soliton. The soliton exhibits an ellipsoidal phase-space motion with period $\tau^{\mathrm{num}}_{\mathrm{c.m.}} \simeq 1.52\tau$ in agreement with the theory, see Eq. (8). The white line reports the theoretical ellipse $H_{\mathrm{c.m.}}$ predicted in Eq. (7). See Movie 3 in [50].

and an incoherent component $\phi(\boldsymbol{x},t)$ of zero mean ($A=\langle\psi\rangle, \phi=\psi-\langle\psi\rangle$)

$$\psi(\boldsymbol{x},t)=A(\boldsymbol{x},t)+\phi(\boldsymbol{x},t).$$

The local spectrum of the IS is the average Wigner transform $n(\boldsymbol{k},\boldsymbol{x},t)=\int\langle\phi(\boldsymbol{x}+\boldsymbol{y}/2,t)\phi^*(\boldsymbol{x}-\boldsymbol{y}/2,t)\rangle\exp(-i\boldsymbol{k}\cdot\boldsymbol{y})d\boldsymbol{y}$. Starting from the SPE (1)–(2), we obtain the result that the soliton and IS components are governed by the coupled SPE and WT-VPE [50]

$$i\partial_t A=-\frac{\alpha}{2}\nabla^2 A+AV, \tag{4}$$

$$\partial_t n(\boldsymbol{k},\boldsymbol{x})+\alpha\boldsymbol{k}\cdot\partial_{\boldsymbol{x}}n(\boldsymbol{k},\boldsymbol{x})-\partial_{\boldsymbol{x}}V\cdot\partial_{\boldsymbol{k}}n(\boldsymbol{k},\boldsymbol{x})=0. \tag{5}$$

Equations (4) and (5) are coupled by the potential $V(\boldsymbol{x},t)=-\gamma U_D*(|A|^2+\rho_{\mathrm{IS}})$, which is the sum of the coherent and incoherent contributions with $\rho_{\mathrm{IS}}(\boldsymbol{x},t)=<|\phi(\boldsymbol{x},t)|^2>=(2\pi)^{-D}\int n(\boldsymbol{k},\boldsymbol{x},t)d\boldsymbol{k}$ the average density of the IS.

Further insight into the coupled SPE and WT-VPE (4)–(5) is obtained through a multiscale expansion in the small parameter $\varepsilon\equiv\tilde{\xi}\ll 1$: $A(\boldsymbol{x},t)=A^{(0)}(\boldsymbol{x},t)$, $n(\boldsymbol{k},\boldsymbol{x},t)=\varepsilon^D n^{(0)}(\varepsilon\boldsymbol{k},\varepsilon\boldsymbol{x},t)$. This scaling gives Eq. (3): $\lambda_c/\Lambda=O(\varepsilon)$, $\ell/\Lambda=O(\varepsilon^{-1})$, $R_S/\Lambda=O(1)$, $\rho_S\sim|A|^2\sim O(1)$, $n\sim O(\varepsilon^D)$, and $\rho_{\mathrm{IS}}\sim O(1)$. Accordingly, we derive an effective SPE (ESPE) for the coherent component [50]

$$i\partial_t A=-\frac{\alpha}{2}\nabla^2 A+V_S A+\gamma q_D\rho_0|\boldsymbol{x}|^2 A, \tag{6}$$

where $V_S(\boldsymbol{x},t)=-\gamma U_D*|A|^2$, $\rho_0(t)=\rho_{\mathrm{IS}}(\boldsymbol{x}=\boldsymbol{0},t)$ is the central average density of the IS, and q_D depends on the dimension, $q_1=1, q_2=\pi/2, q_3=2\pi/3$. The ESPE (6) reveals that the coherent (soliton) component experiences its self-gravitational potential V_S and an unexpected parabolic trapping potential due to the IS.

Dynamics of hidden solitons in D dimension.—We describe the general form of the spinning binary soliton by using the variational approach (for $D=1$, 3). We consider the Lagrangian of the ESPE (6) with the Gaussian ansatz

$$A(\boldsymbol{x},t)=\sum_{j=1}^{2}a_j(t)\exp\left(-\frac{|\boldsymbol{x}-\boldsymbol{x}_{o,j}(t)|^2}{2R_{S,j}^2(t)}+i\Phi_j(\boldsymbol{x},t)\right),$$

where $\Phi_j(\boldsymbol{x},t)=\boldsymbol{k}_{o,j}(t)\cdot[\boldsymbol{x}-\boldsymbol{x}_{o,j}(t)]+b_j(t)|\boldsymbol{x}-\boldsymbol{x}_{o,j}(t)|^2+\nu_j(t)$. The evolution of the phase-space coordinates of the jth soliton $[\boldsymbol{x}_{o,j}(t),\boldsymbol{k}_{o,j}(t)]$ are obtained from the principle of least action through the Euler-Lagrange equations [50].

Ellipsoidal motion of the center of mass.—The dynamics of the binary soliton can be decomposed into the motion of the center of mass (c.m.) and the mutual relative displacement of the two solitons in the c.m. reference frame. The equations for the c.m., $\boldsymbol{X}_{\mathrm{c.m.}}=(M_{S,1}\boldsymbol{x}_{o,1}+M_{S,2}\boldsymbol{x}_{o,2})/(M_{S,1}+M_{S,2})$, and $\boldsymbol{K}_{\mathrm{c.m.}}=(M_{S,1}\boldsymbol{k}_{o,1}+M_{S,2}\boldsymbol{k}_{o,2})/(M_{S,1}+M_{S,2})$, can be recast in Hamiltonian form $\partial_t\boldsymbol{X}_{\mathrm{c.m.}}=\partial_{\boldsymbol{K}_{\mathrm{c.m.}}}H_{\mathrm{c.m.}}$, $\partial_t\boldsymbol{K}_{\mathrm{c.m.}}=-\partial_{\boldsymbol{X}_{\mathrm{c.m.}}}H_{\mathrm{c.m.}}$ with

$$H_{\mathrm{c.m.}}=q_D\gamma\rho_0|\boldsymbol{X}_{\mathrm{c.m.}}|^2+\frac{\alpha}{2}|\boldsymbol{K}_{\mathrm{c.m.}}|^2. \tag{7}$$

The barycenter of the binary soliton then exhibits a periodic ellipsoidal motion in phase space with a revolution period

$$\tau_{\mathrm{c.m.}}=\sqrt{2}\pi/\sqrt{\alpha\gamma q_D\rho_0}. \tag{8}$$

First, we comment the case $D=1$ through the SPE simulation reported in Fig. 2: The average density $\rho_0=(3.9\pm0.2)\bar{\rho}$ gives $\tau_{\mathrm{c.m.}}=(1.56\pm0.04)\tau$ from (8), which is in agreement with the simulation ($\tau_{\mathrm{c.m.}}^{\mathrm{num}}\simeq 1.56\tau$).

The revolution period (8) also applies to the ellipsoidal motion of a single soliton where the c.m. coincides with the soliton position. In Fig. 3, $\rho_0=(4.2\pm0.2)\bar{\rho}$ gives $\tau_{\mathrm{c.m.}}=(1.52\pm0.04)\tau$, which is in agreement with the SPE simulation ($\tau_{\mathrm{c.m.}}^{\mathrm{num}}\simeq 1.52\tau$) [50].

For $D=3$, the dynamics $\boldsymbol{X}_{\mathrm{c.m.}}(t)$ lies in a plane and exhibits an ellipsoidal motion: $\boldsymbol{X}_{\mathrm{c.m.}}=[\mathcal{R}(\theta)\cos\theta, \mathcal{R}(\theta)\sin\theta, 0]$ where $\mathcal{R}(\theta)=(w_-\cos^2\theta+w_+\sin^2\theta)^{-1/2}c_1^{-1/4}$ with $\theta(t)=\arctan[w_-\tan(c_o\sqrt{c_1}t)]$, $c_1=2q_3\alpha\gamma\rho_0/c_o^2$, $w_\pm$, and $c_{o,1}$ being constants of the motion [50].

Revolution period for the binary soliton.—The Hamiltonian equations governing the relative position of the binary soliton, namely, $\boldsymbol{X}_o=\boldsymbol{x}_{o,1}-\boldsymbol{x}_{o,2}$, $\boldsymbol{K}_o=\boldsymbol{k}_{o,1}-\boldsymbol{k}_{o,2}$, read $\partial_t\boldsymbol{X}_o=\partial_{\boldsymbol{K}_o}H_o$, $\partial_t\boldsymbol{K}_o=-\partial_{\boldsymbol{X}_o}H_o$, with

$$H_o=q_D\gamma\rho_0|\boldsymbol{X}_o|^2+\gamma(M_{S,1}+M_{S,2})|\boldsymbol{X}_o|^{2-D}+\frac{\alpha}{2}|\boldsymbol{K}_o|^2. \tag{9}$$

For $D=1$, the phase-space trajectory is reported in Fig. 2. The spinning binary soliton exhibits a revolution period [50]

$$\tau_{\mathrm{bin}}=4\sqrt{2}\arcsin(\sqrt{\beta/2})/\sqrt{\alpha\gamma\rho_0}, \tag{10}$$

where $\beta=1-(M_{S,1}+M_{S,2})/\sqrt{\chi}$, and $\chi=(M_{S,1}+M_{S,2})^2+4\rho_0 d(\rho_0 d+M_{S,1}+M_{S,2})$, with d the maximal soliton distance. The spinning for the binary soliton is always faster than for a single soliton ($\tau_{\mathrm{bin}}<\tau_{\mathrm{c.m.}}$), as confirmed by the SPE simulation in Fig. 2 where $\tau_{\mathrm{bin}}=(1.43\pm0.04)\tau$ is in agreement with the simulation ($\tau_{\mathrm{bin}}^{\mathrm{num}}\simeq 1.43\tau$).

For $D=3$, the motion of the binary soliton lies in a plane: $\boldsymbol{X}_o=[\mathcal{R}(\theta)\cos\theta, \mathcal{R}(\theta)\sin\theta, 0]$, where $u(\theta)=1/\mathcal{R}(\theta)$ is the solution of $\partial_\theta^2 u+u=c_1/u^3+c_2$, where $\partial_t\theta=c_o\mathcal{R}(\theta)^{-2}$, $c_{o,1,2}$ being constants of the motion. The orbit $\boldsymbol{X}_o$ is not closed, in general, and the motion in the plane exhibits a perihelion precession [50].

Discussion and perspectives.—We have reported a novel regime of the SPE characterized by hidden soliton states that are trapped and stabilized by the IS. The regime of hidden solitons can be observed in highly nonlocal nonlinear optics experiments with long-range thermal nonlinearities, in line with the recent emulations of rotating Bose stars, or gravitational lensing and redshifts [32,33]. The hidden solitons can be experimentally unveiled through the measurement of the optical spectrogram [50,55].

Aside from its relevance to bosonic models of fuzzy dark matter, our work sheds new light on the quantum-to-classical (or SPE to VPE) correspondence in the limit $\hbar/m \to 0$: The hidden solitons revealed here refer to the latest residual quantum correction preceding the purely classical limit provided by the VPE.

The authors are grateful to J. Niemeyer for drawing our attention to this problem and for the fruitful discussions and suggestions during the early stage of this work. The authors also thank S. Rica and S. Nazarenko for valuable comments. We acknowledge financial support from the French ANR under Grant No. ANR-19-CE46-0007 (Project ICCI), French program "Investissement d'Avenir," Project No. ISITE-BFC-299 (ANR-15 IDEX-0003); H2020 Marie Sklodowska-Curie Actions (MSCA-COFUND) (MULTIPLY Project No. 713694).

[1] V. Zakharov, A. Pushkarev, V. Shvets, and V. Yan'kov, Soliton turbulence, JETP Lett. **48**, 83 (1988).
[2] R. Rumpf and A. C. Newell, Coherent Structures and Entropy in Constrained, Modulationally Unstable, Nonintegrable Systems, Phys. Rev. Lett. **87**, 054102 (2001).
[3] R. Jordan and C. Josserand, Self-organization in nonlinear wave turbulence, Phys. Rev. E **61**, 1527 (2000).
[4] V. Zakharov, F. Dias, and A. Pushkarev, One-dimensional wave turbulence, Phys. Rep. **398**, 1 (2004).
[5] J. Laurie, U. Bortolozzo, S. Nazarenko, and S. Residori, One-dimensional optical wave turbulence: Experiment and theory, Phys. Rep. **514**, 121 (2012).
[6] S. Nazarenko, *Wave Turbulence*, Lectures Notes in Physics (Springer, New York, 2011).
[7] A. C. Newell and B. Rumpf, Wave turbulence, Annu. Rev. Fluid Mech. **43**, 59 (2011).
[8] A. C. Newell, S. Nazarenko, and L. Biven, Wave turbulence and intermittency, Physica (Amsterdam) **152D–153D**, 520 (2001).
[9] A. Campa, T. Dauxois, D. Fanelli, and S. Ruffo, *Physics of long-range interacting systems* (Oxford University Press, New York, 2014).
[10] L. Diósi, Gravitation and quantum-mechanical localization of macro-objects, Phys. Lett. **105A**, 199 (1984).
[11] R. Penrose, On gravity's role in quantum state reduction., Gen. Relativ. Gravit. **28**, 581 (1996).
[12] R. Ruffini and S. Bonazzola, Systems of self-gravitating particles in general relativity and the concept of an equation of state, Phys. Rev. **187**, 1767 (1969).
[13] D. Giulini and A. Grossardt, The Schrödinger-Newton equation as a non-relativistic limit of self-gravitating Klein-Gordon and Dirac fields, Classical Quantum Gravity **29**, 215010 (2012).
[14] P.-H. Chavanis, Self-gravitating Bose-Einstein condensates, edited by X. Calmet, in *Quantum Aspects of Black Holes* (Springer International Publishing, Cham, 2015), Chap. 6, pp. 151–194.
[15] P. Jetzer, Bosons stars, Phys. Rep. **220**, 163 (1992).
[16] P.-H. Chavanis, Mass-radius relation of Newtonian self-gravitating Bose-Einstein condensates with short-range interactions. I. Analytical results, Phys. Rev. D **84**, 043531 (2011).
[17] A. Suárez, V. H. Robles, and T. Matos, A review on the scalar field/Bose-Einstein condensate dark matter model, in *Accelerated Cosmic Expansion*, edited by C. Moreno González, J. E. Madriz Aguilar, and L. M. Reyes Barrera (Springer International, Cham, 2014), pp. 107–142.
[18] D. H. Weinberg, J. S. Bullock, F. Governato, R. Kuzio de Naray, and A. H. G. Peter, Cold dark matter: Controversies on small scales, Proc. Natl. Acad. Sci. U.S.A. **112**, 12249 (2015).
[19] L. Hui, J. P. Ostriker, S. Tremaine, and E. Witten, Ultralight scalars as cosmological dark matter, Phys. Rev. D **95**, 043541 (2017).
[20] D. J. E. Marsh, Axion cosmology, Phys. Rep. **643**, 1 (2016).
[21] E. Braaten and H. Zhang, The physics of axion stars, Rev. Mod. Phys. **91**, 041002 (2019).
[22] J. C. Niemeyer, Small-scale structure of fuzzy and axion-like dark matter, Prog. Part. Nucl. Phys. **113**, 103787 (2020).
[23] H.-Y. Schive, T. Chiueh, and T. Broadhurst, Cosmic structure as the quantum interference of a coherent dark wave, Nat. Phys. **10**, 496 (2014).
[24] H.-Y. Schive, M.-H. Liao, T.-P. Woo, S.-K. Wong, T. Chiueh, T. Broadhurst, and W.-Y. P. Hwang, Understanding the Core-Halo Relation of Quantum Wave Dark Matter from 3D Simulations, Phys. Rev. Lett. **113**, 261302 (2014).
[25] B. Schwabe, J. C. Niemeyer, and J. F. Engels, Simulations of solitonic core mergers in ultralight axion dark matter cosmologies, Phys. Rev. D **94**, 043513 (2016).
[26] P. Mocz, M. Vogelsberger, V. H. Robles, J. Zavala, M. Boylan-Kolchin, A. Fialkov, and L. Hernquist, Galaxy formation with BECDM ? I. Turbulence and relaxation of idealized haloes, Mon. Not. R. Astron. Soc. **471**, 4559 (2017).
[27] P. Mocz, L. Lancaster, A. Fialkov, F. Becerra, and P.-H. Chavanis, Schrödinger-Poisson–Vlasov-Poisson correspondence, Phys. Rev. D **97**, 083519 (2018).
[28] N. Bar, D. Blas, K. Blum, and S. Sibiryakov, Galactic rotation curves versus ultralight dark matter: Implications of the soliton-host halo relation, Phys. Rev. D **98**, 083027 (2018).
[29] P. Mocz, A. Fialkov, M. Vogelsberger, F. Becerra, M. A. Amin, S. Bose, M. Boylan-Kolchin, P.-H. Chavanis, L. Hernquist, L. Lancaster, F. Marinacci, V. H. Robles, and J. Zavala, First Star-Forming Structures in Fuzzy Cosmic Filaments, Phys. Rev. Lett. **123**, 141301 (2019).

[30] H.-Yu Schive, T. Chiueh, and T. Broadhurst, Soliton Random Walk and the Cluster-Stripping Problem in Ultralight Dark Matter, Phys. Rev. Lett. **124**, 201301 (2020).

[31] *Analogue Gravity Phenomenology*, Lectures Notes in Physics Vol. 870, edited by D. Faccio, F. Belgiorno, S. Cacciatori, V. Gorini, S. Liberati, and U. Moschella (Springer, New York, 2013).

[32] R. Bekenstein, R. Schley, M. Mutzafi, C. Rotschild, and M. Segev, Optical simulations of gravitational effects in the Newton-Schrödinger system, Nat. Phys. **11**, 872 (2015).

[33] T. Roger, C. Maitland, K. Wilson, N. Westerberg, D. Vocke, E. M. Wright, and D. Faccio, Optical analogues of the Newton-Schrödinger equation and boson star evolution, Nat. Commun. **7**, 13492 (2016).

[34] F. Marino, Massive phonons and gravitational dynamics in a photon-fluid model, Phys. Rev. A **100**, 063825 (2019).

[35] J. Skipp, V. L'vov, and S. Nazarenko, Wave turbulence in self-gravitating Bose gases and nonlocal nonlinear optics, Phys. Rev. A **102**, 043318 (2020).

[36] A. Paredes, D. N. Olivieri, and H. Michinel, From optics to dark matter: A review on nonlinear Schrödinger-Poisson systems, Physica (Amsterdam) **403D**, 132301 (2020).

[37] M. Segev and D. Christodoulides, Incoherent solitons, edited by S. Trillo and W. Torruellas, in *Spatial Solitons* (Springer, Berlin, 2001).

[38] Y. Kivshar and G. P. Agrawal, *Optical Solitons: From Fibers to Photonic Crystals* (Academic Press, Boston, 2003).

[39] A. Picozzi, J. Garnier, T. Hansson, P. Suret, S. Randoux, G. Millot, and D. N. Christodoulides, Optical wave turbulence: Toward a unified nonequilibrium thermodynamic formulation of statistical nonlinear optics, Phys. Rep. **542**, 1 (2014).

[40] O. Cohen, H. Buljan, T. Schwartz, J. W. Fleischer, and M. Segev, Incoherent solitons in instantaneous nonlocal nonlinear media, Phys. Rev. E **73**, 015601(R) (2006).

[41] C. Rotschild, T. Schwartz, O. Cohen, and M. Segev, Incoherent spatial solitons in effectively-instantaneous nonlocal nonlinear media, Nat. Photonics **2**, 371 (2008).

[42] C. Rotschild, B. Alfassi, O. Cohen, and M. Segev, Long-range interactions between optical solitons, Nat. Phys. **2**, 769 (2006).

[43] S. Skupin, M. Saffman, and W. Krolikowski, Nonlocal Stabilization of Nonlinear Beams in a Self-Focusing Atomic Vapor, Phys. Rev. Lett. **98**, 263902 (2007).

[44] M. Peccianti, C. Conti, G. Assanto, A. De Luca, and C. Umeton, Routing of anisotropic spatial solitons and modulational instability in liquid crystals, Nature (London) **432**, 733 (2004).

[45] C. Rotschild, O. Cohen, O. Manela, M. Segev, and T. Carmon, Solitons in Nonlinear Media with an Infinite Range of Nonlocality: First Observation of Coherent Elliptic Solitons and of Vortex-Ring Solitons, Phys. Rev. Lett. **95**, 213904 (2005).

[46] G. Marcucci, D. Pierangeli, S. Gentilini, N. Ghofraniha, Z. Chen, and C. Conti, Optical spatial shock waves in nonlocal nonlinear media, Adv. Phys. X **4**, 1662733 (2019).

[47] M. A. Baranov, Theoretical progress in many-body physics with ultracold dipolar gases, Phys. Rep. **464**, 71 (2008).

[48] D. G. Levkov, A. G. Panin, and I. I. Tkachev, Gravitational Bose-Einstein Condensation in the Kinetic Regime, Phys. Rev. Lett. **121**, 151301 (2018).

[49] J. Chen, X. Du, E. W. Lentz, D. J. E. Marsh, and J. C. Niemeyer, New insights into the formation and growth of boson stars in dark matter halos, arXiv:2011.01333.

[50] See Supplemental Material at http://link.aps.org/supplemental/10.1103/PhysRevLett.127.014101 which reports the derivation of the ESPE (6), the derivation of the revolution periods for the center of mass [Eq. (8)], and for the binary soliton system [Eq. (10)], which includes Refs. [51–53]. It also reports three animations (Movies 1–3) corresponding to the SPE numerical simulations in Figs. 1–3.

[51] J. Garnier, J.-P. Ayanides, and O. Morice, Propagation of partially coherent light with the Maxwell-Debye equation, J. Opt. Soc. Am. B **20**, 1409 (2003).

[52] C. Uhlemann, M. Kopp, and T. Haugg, Schrödinger method as N—body double and UV completion of dust, Phys. Rev. D **90**, 023517 (2014).

[53] B. A. Malomed, Variational methods in nonlinear fiber optics and related fields, Prog. Opt. **43**, 71 (2002).

[54] M. Yu. Khlopov, B. A. Malomed, and Ya. B. Zeldovich, Gravitational instability of scalar fields and formation of primordial black holes, Mon. Not. R. Astron. Soc. **215**, 575 (1985).

[55] L. Waller, G. Situ, and J. W. Fleischer, Phase-space measurement and coherence synthesis of optical beams, Nat. Photonics **6**, 474 (2012).

[56] V. E. Zakharov, V. S. L'vov, and G. Falkovich, *Kolmogorov Spectra of Turbulence I* (Springer, Berlin, 1992).

[57] A. Picozzi and J. Garnier, Incoherent Soliton Turbulence in Nonlocal Nonlinear Media, Phys. Rev. Lett. **107**, 233901 (2011).

[58] A. C. Newell, B. Rumpf, and V. E. Zakharov, Spontaneous Breaking of the Spatial Homogeneity Symmetry in Wave Turbulence, Phys. Rev. Lett. **108**, 194502 (2012).

[59] G. Xu, D. Vocke, D. Faccio, J. Garnier, T. Rogers, S. Trillo, and A. Picozzi, From coherent shocklets to giant collective incoherent shock waves in nonlocal turbulent flows, Nat. Commun. **6**, 8131 (2015).

[60] G. Xu, J. Garnier, D. Faccio, S. Trillo, and A. Picozzi, Incoherent shock waves in long-range optical turbulence, Physica (Amsterdam) **333D**, 310 (2016).

[61] S. K. Turitsyn, S. A. Babin, E. G. Turitsyna, G. E. Falkovich, E. Podivilov, and D. Churkin, Optical wave turbulence, in *Wave Turbulence*, edited by V. Shira and S. Nazarenko, World Scientific Series on Nonlinear Science Series A Vol. 83 (World Scientific, Singapore, 2013).

[62] M. Onorato, S. Residori, U. Bortolozzo, A. Montina, and F. T. Arecchi, Rogue waves and their generating mechanisms in different physical contexts, Phys. Rep. **528**, 47 (2013).

[63] V. S. Lvov and A. M. Rubenchik, Spatially non-uniform singular weak turbulence spectra, Sov. Phys. JETP **45**, 67 (1977).

[64] A. I. Dyachenko, S. V. Nazarenko, and V. E. Zakharov, Wave-vortex dynamics in drift and β—plane turbulence, Phys. Lett. A **165**, 330 (1992).

[65] V. E. Zakharov, S. L. Musher, and A. M. Rubenchik, Hamiltonian approach to the description of non-linear plasma phenomena, Phys. Rep. **129**, 285 (1985).